

A general system of images for regularized Stokeslets and other elements near a plane wall



Ricardo Cortez^{a,*}, Douglas Varela^b

^a Mathematic Department, Tulane University, United States

^b DVC Academic Consulting, San Pablo, CA, United States

ARTICLE INFO

Article history:

Received 17 July 2014

Received in revised form 31 December 2014

Accepted 12 January 2015

Available online 17 January 2015

Keywords:

Stokeslet

Stokes flow

Method of images

ABSTRACT

We derive a general system of images for regularized sources, Stokeslets, and other related elements starting from an arbitrary regularization kernel (blob) used in the simulation of Stokes flows in three dimensions bounded by a plane. This generalizes previous work in which the image system for a Stokeslet had been derived for one specific blob. The significance of this generalization is that recent work on regularization methods requires the use of blobs designed to satisfy certain properties, such as zero moment conditions and fast decay, and thus it is absolutely necessary to have the system of images starting from an arbitrary blob. The system of images for a regularized element consists of a set of several elements, usually of higher order, that produce a flow that is zero at the bounding plane. In order for the resultant flow to vanish analytically at the wall, two different but related blobs must be used. For any given blob, we provide the formula for the companion blob that accomplishes the cancellation and we derive a systematic way to compute the image system of regularized Stokeslets, sources and dipoles. Other elements can be derived from these. By taking the limit as the regularization parameter approaches zero, the system of images for the corresponding singular elements is found.

© 2015 Elsevier Inc. All rights reserved.

1. Introduction

There are many fluid flow problems in the sciences and engineering that are solved through the use of singularity solutions distributed along the surface of bodies interacting with the fluid. In biological flows, for example, the forces imparted on the fluid by flagella, cilia, cell bodies, and other objects are often modeled as Stokeslet distributions on the surfaces affecting the fluid motion. This approach relies on the fact that a surface distribution of Stokeslets is integrable. The Stokeslet can be differentiated to produce additional singularity solutions of Stokes equations such as the rotlet, stresslet, dipole, quadrupole, etc. Among them, the rotlet has been used substantially since it represents the fluid motion due to a point-torque and is needed to balance the angular momentum in propulsive mechanisms of microorganisms [8]. In applications such as the swimming motion of self-propelled organisms [17,9,27,10,29] and the conical rotation of nodal cilia [35], the stresslet flow is known to appear.

Unlike the Stokeslet, the singularities that come from its derivatives are generally no longer integrable when distributed over surfaces. Similarly, Stokeslets distributed along curves or scattered points produce infinite velocities, so the singularities must be removed by computing the principal value of the integrals, for example. The method of regularized Stokeslet

* Corresponding author.

E-mail addresses: rcortez@tulane.edu (R. Cortez), douglas.varela@davinci-camp.com (D. Varela).

[14,15] was developed to remove the Stokeslet singularity by smoothing the kernels. Since its introduction in 2001, this method has been very useful for small-scale biological flow applications such as the swimming motions of microorganisms, cell growth, and other microscopic phenomena. It has been used for biofilm/fluid interactions [12,11], for microfiltration as a method for removing particulate matter [13], for spirochete motility studies [15] and the simulation of bundling flagella [18], to model swimming flagella [26], to understand forces of self-propelled microswimmers [23], to model a human sperm motility [21], to study asymmetric peristaltic pumping in three dimensions [2], to determine the rotational velocity of superhelical bodies being towed through a very viscous fluid [22], and to study hydrodynamic interactions that cause synchronization between rotating paddles in a viscous fluid [31]. Improvements on the implementation of the method have also been proposed [7,34,3].

The regularized Stokeslet is the velocity field that solves the incompressible Stokes equations with external forcing

$$\nabla p = \Delta \mathbf{u} + \mathbf{f}, \quad \nabla \cdot \mathbf{u} = 0 \quad (1)$$

with forcing of the form

$$\mathbf{f}(\mathbf{x}) = \sum_{k=1}^N \mathbf{f}_k \phi_\delta(\mathbf{x} - \mathbf{x}_k) \quad (2)$$

where $\phi_\delta(\mathbf{x})$ is concentrated in a small neighborhood of the origin whose size is determined by the parameter δ . The blob ϕ_δ is assumed to be a radially-symmetric, smooth approximation to a delta-distribution, so we require at a minimum that its total volume integral be one. The exact solution of the Stokes equations (1) with forcing term in Eq. (2) can be found analytically, leading to a regularized Stokeslet, which is bounded everywhere. It also has the property that as the regularization parameter δ approaches zero, the expression converges to the well-known singular counterpart [14]. Once the regularized Stokeslet is known, other solutions can be derived by differentiation, leading to regularized dipoles, rotlets, stresslets, etc.

Interesting problems involve flows in the vicinity of a plane wall. Observations of microorganisms swimming in solutions are often made near the bottom glass plate of a container [10], where the flows generated by the organism's flagella are affected by the presence of the wall. Similarly, cilia beat next to a boundary that affects the overall flow. In order to include the zero-velocity boundary condition on a plane, a system of images for regularized Stokeslets was presented in [1]. Given the forces in Eq. (2), the image of \mathbf{x}_k is its reflection about the plane wall. By placing a set of regularized elements at the image point, it is possible to cancel analytically the flow on the wall. Early work on the image system of singular Stokeslets appears in [5,6] where Fourier transforms were used for the derivation of the images for a Stokeslet, rotlet, source, and (Stokeslet) doublet. By differentiating with respect to the pole, Pozrikidis [30, p. 197] also derived the image systems for the Stokeslet, source and dipole.

The image system for regularized Stokeslets presented in [1] was derived specifically for the algebraic blob

$$\phi_\delta(\mathbf{x}) = \frac{15\delta^4}{8\pi(|\mathbf{x}|^2 + \delta^2)^{7/2}}. \quad (3)$$

This image system included a regularized Stokeslet, doublet, dipole and rotlets. It turned out that some of those element had to be derived from a “companion” blob in order to achieve the necessary cancellation of terms. While the regularized image system has been useful in many applications of microorganism motility, nano motors, sperm motility, cilia dynamics, and more [34,10,9,21,20,35,24,33], it is clear that a more general theory is needed to allow the use of specialized blobs in the regularized Stokeslet.

For example, higher accuracy in computing the Stokeslet flow due to a moving object may be achieved if the blobs used to regularize the surface forces satisfy certain moment conditions of the form $\int_0^\infty r^{m+2} \phi_\delta(r) dr = 0$ for integers $m \geq 1$ (see [4,28]). Recent work on periodic arrays of regularized Stokeslets [25] considers a force \mathbf{f} applied at \mathbf{x}_0 in a box domain $[0, L]^3$ and the solution of Eq. (1) written as $\mathbf{u}(\mathbf{x}) = S^\delta(\mathbf{x}, \mathbf{x}_0)\mathbf{f} + \sum_{\mathbf{n} \neq 0} S^\delta(\mathbf{x}, \mathbf{x}_0 + \mathbf{n}L)\mathbf{f}$, where \mathbf{n} is a triple index representing the periodic copies of the force. This can be written as

$$\mathbf{u}(\mathbf{x}) = S^\delta(\mathbf{x}, \mathbf{x}_0)\mathbf{f} + \sum_{\mathbf{n} \neq 0} [S^\delta(\mathbf{x}, \mathbf{x}_0 + \mathbf{n}L) - S^0(\mathbf{x}, \mathbf{x}_0 + \mathbf{n}L)]\mathbf{f} + \sum_{\mathbf{n} \neq 0} S^0(\mathbf{x}, \mathbf{x}_0 + \mathbf{n}L)\mathbf{f}$$

where S^0 represents the singular Stokeslet. Since the last term can be treated using an Ewald splitting technique; the efficiency of the computation depends on the fast approximation of the first sum on the right side. This requires the use of Gaussian blobs so that the first sum is local in space. The blob in Eq. (3) cannot be used in these situations. This technique has been extended to doubly-periodic arrays of forces (in x and y) and unbounded space in the z -direction [16]. The further extension of the doubly-periodic case to include the plane wall $z = z_0$ can be accomplished with Gaussian blobs.

Here, we generalize the Stokeslet image system by deriving it for an arbitrary blob. A formula for the “companion” blob, which is used in some of the image elements, is derived. We also derive the image system for a regularized source (or sink) so that the image systems for other elements (e.g. doublets and dipoles) can be obtained by differentiation with respect to the pole [30].

2. The regularized elements in free space

Let $\phi(r)$ be any blob and define the corresponding regularized Green's function $G(r)$ as a smooth solution of $\Delta G = \phi$ in \mathbb{R}^3 subject to the condition $G(r) \rightarrow 0$ as $r \rightarrow \infty$. Also define the corresponding regularized biharmonic function $B(r)$ as a smooth solution of $\Delta B = G$. Note that since the blob is radially symmetric, this implies that $(r^2 G'(r))' = r^2 \phi(r)$ and $(r^2 B'(r))' = r^2 G(r)$.

2.1. Regularized source

We consider the Stokes equations (1) with no external forcing but with divergence $\nabla \cdot \mathbf{u} = m\phi(|\mathbf{x}|)$. Taking the divergence of the Stokes equation we have that

$$\Delta p = m \Delta \phi \Rightarrow p(\mathbf{x}) = m \phi(|\mathbf{x}|).$$

Other solutions differ from this one by a harmonic function but by requiring that the pressure be bounded as $|\mathbf{x}| \rightarrow \infty$, all solutions differ by a constant that can be taken to be zero. Then the velocity satisfies

$$\Delta \mathbf{u} = \nabla p = m \nabla \phi \Rightarrow \mathbf{u}(\mathbf{x}) = m \nabla G(\mathbf{x}).$$

Since G is radially symmetric, the velocity can be written as

$$\mathbf{u}(\mathbf{x}) = m \Sigma(r) \mathbf{x}, \quad \text{where } \Sigma(r) = \frac{G'(r)}{r} \tag{4}$$

and $r = |\mathbf{x}|$.

2.2. Regularized Stokeslet

Taking the divergence of Eq. (1) with forcing $\mathbf{f}\phi(|\mathbf{x}|)$ we have that

$$\Delta p = \mathbf{f} \cdot \nabla \phi \Rightarrow p(\mathbf{x}) = (\mathbf{f} \cdot \nabla) G(|\mathbf{x}|).$$

Then the velocity satisfies

$$\Delta \mathbf{u} = \nabla p - \mathbf{f}\phi = (\mathbf{f} \cdot \nabla) \nabla G - \mathbf{f}\phi \Rightarrow \mathbf{u}(\mathbf{x}) = (\mathbf{f} \cdot \nabla) \nabla B(r) - \mathbf{f}G(r)$$

where $r = |\mathbf{x}|$. Using the radial symmetry of G and B , the velocity can be written as

$$\mathbf{u}(\mathbf{x}) = \mathbf{f} H_1(r) + (\mathbf{f} \cdot \mathbf{x}) \mathbf{x} H_2(r)$$

where

$$H_1 = \frac{B'(r)}{r} - G(r) \quad \text{and} \quad H_2 = \frac{rB''(r) - B'(r)}{r^3} \tag{5}$$

2.3. Regularized doublet

Let the Stokeslet velocity components be given in component form by

$$u_i \equiv S_{ij} f_j = [H_1(r) \delta_{ij} + x_i x_j H_2(r)] f_j$$

then the doublet kernel Δ_{ijk} is defined as

$$\Delta_{ijk} = \frac{\partial}{\partial x_k} S_{ij} = \frac{H_1'}{r} x_k \delta_{ij} + H_2 (\delta_{ik} x_j + \delta_{jk} x_i) + \frac{H_2'}{r} x_i x_j x_k$$

The expression for the doublet can be split into a part that is symmetric with respect to the subscripts j and k , and the antisymmetric part. These are related to a *stresslet* and *rotlet*, respectively. We write the above expression as

$$\Delta_{ijk} = \left\{ H_2 \delta_{jk} x_i + \frac{H_2'}{r} x_i x_j x_k + \frac{1}{2} \left(H_2 + \frac{H_1'}{r} \right) (\delta_{ik} x_j + \delta_{ij} x_k) \right\} + \frac{1}{2} \left(H_2 - \frac{H_1'}{r} \right) (\delta_{ik} x_j - \delta_{ij} x_k)$$

The terms in curly braces is symmetric and the last term is antisymmetric. From the definitions of H_1 and H_2 in the previous subsection, we simplify the antisymmetric term to get

$$\Delta_{ijk} = \left\{ H_2 \delta_{jk} x_i + \frac{H_2'}{r} x_i x_j x_k + \frac{1}{2} \left(H_2 + \frac{H_1'}{r} \right) (\delta_{ik} x_j + \delta_{ij} x_k) \right\} + \frac{1}{2} \frac{G'}{r} (\delta_{ik} x_j - \delta_{ij} x_k)$$

2.3.1. Regularized rotlet

The rotlet comes from applying the regularized doublet to an antisymmetric matrix, A_{jk} . Based on the decomposition of the doublet, this is

$$u_i \equiv \Delta_{ijk} A_{jk} = \frac{1}{2} \frac{G'}{r} (\delta_{ik} x_j - \delta_{ij} x_k) A_{jk} = -\frac{G'}{r} x_k A_{ik}.$$

Since the matrix has only 3 independent elements, we may exploit its symmetry to write $A_{ik} = -\epsilon_{ijk} \bar{L}_j$ for some vector \bar{L} . Then the rotlet velocity is

$$u_i \equiv \mathcal{R}_{ij} \bar{L}_j = \left[\frac{G'}{r} \epsilon_{ij\ell} x_\ell \right] \bar{L}_j$$

where \bar{L} is the rotlet strength. This result is also found in [18].

2.3.2. Regularized stresslet

If we apply the regularized doublet to a symmetric matrix, Z_{jk} , the result is

$$\begin{aligned} \Delta_{ijk} Z_{jk} &= \left\{ H_2 \delta_{jk} x_i + \frac{H'_2}{r} x_i x_j x_k + \frac{1}{2} \left(H_2 + \frac{H'_1}{r} \right) (\delta_{ik} x_j + \delta_{ij} x_k) \right\} Z_{jk} \\ &= H_2 x_i (\delta_{jk} Z_{jk}) + \frac{H'_2}{r} x_i x_j x_k Z_{jk} + \left(H_2 + \frac{H'_1}{r} \right) x_j Z_{ij}. \end{aligned} \quad (6)$$

In Section 4 we discuss how the first term can be interpreted as a regularized source, so we define the stresslet velocity as

$$u_i \equiv T_{ijk} Z_{ik} = \frac{H'_2}{r} x_i x_j x_k Z_{jk} + \left(H_2 + \frac{H'_1}{r} \right) x_k Z_{ik}.$$

We point out that the regularization introduces terms in the derived expressions that are not present in the well-known singular versions. For example, the term $H_2(r) + H'_1(r)/r$ vanishes identically in the singular case but not in the regularized case.

2.4. Regularized dipole

The regularized dipole velocity is derived as the negative Laplacian of the regularized Stokeslet. The result is $\mathbf{u}(\mathbf{x}) = \mathbf{f}\phi(|\mathbf{x}|) - (\mathbf{f} \cdot \nabla) \nabla G(\mathbf{x})$ which we write as

$$u_i \equiv D_{ij} f_j = [D_1(r) \delta_{ij} + x_i x_j D_2(r)] f_j$$

where

$$D_1 = \phi(r) - \frac{G'(r)}{r} \quad \text{and} \quad D_2 = -\frac{1}{r} \left(\frac{G'(r)}{r} \right)'. \quad (7)$$

2.5. Other elements

We mention three more elements that will be needed in some of the image systems.

Regularized quadrupole: The quadrupole kernel Q_{ijk} is defined as a derivative of the dipole

$$Q_{ijk} = \frac{\partial}{\partial x_k} D_{ij} = \frac{D'_1}{r} x_k \delta_{ij} + D_2 (\delta_{ik} x_j + \delta_{jk} x_i) + \frac{D'_2}{r} x_i x_j x_k.$$

Regularized rotlet double: The rotlet double kernel Θ_{ijk} is defined as the derivative of a rotlet

$$\Theta_{ijk} = \frac{\partial}{\partial x_k} \mathcal{R}_{ij} = \frac{\mathcal{R}'}{r} \epsilon_{ij\ell} x_\ell x_k + \mathcal{R} \epsilon_{ijk}.$$

Regularized Stokeslet quadrupole: The Stokeslet quadrupole kernel $S_{ijk\ell}^Q$ is defined as

$$S_{ijk\ell}^Q = \frac{\partial}{\partial x_\ell} \Delta_{ijk}.$$

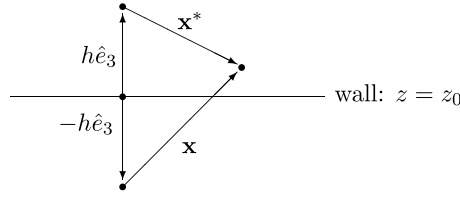


Fig. 1. Schematic of the geometry and notation near the wall. The original element is centered at the point above the wall; the image point is below the wall.

Table 1

Examples of algebraic, exponential and Gaussian blob pairs ϕ_d and ϕ_s . The top row corresponds to the blobs used in [1].

Dipole/source blob	Stokeslet blob
$\phi_d(r) = \frac{3\delta^2}{4\pi(r^2 + \delta^2)^{5/2}}$	$\phi_s(r) = \frac{15\delta^4}{8\pi(r^2 + \delta^2)^{7/2}}$
$\phi_d(r) = \frac{(r + \delta) \exp(-r/\delta)}{32\pi\delta^4}$	$\phi_s(r) = \frac{(5\delta^2 + 5\delta r - r^2) \exp(-r/\delta)}{64\pi\delta^4}$
$\phi_d(r) = \frac{\exp(-r^2/\delta^2)}{\pi^{3/2}\delta^3}$	$\phi_s(r) = \frac{(5\delta^2 - 2r^2) \exp(-r^2/\delta^2)}{2\pi^{3/2}\delta^5}$

3. Motivation for using two different blobs

From now on, we will consider an infinite plane wall parallel to the xy -plane at $z = z_0$. Let \mathbf{x}^* represent the vector from the location of the regularized Stokeslet to an evaluation point and let \mathbf{x} be the vector from the image point to the same evaluation point. We define h to be the distance from the regularized Stokeslet to the wall (see Fig. 1).

The components of the vectors \mathbf{x} and \mathbf{x}^* satisfy

$$x_i^* = x_i - 2h\delta_{i3} \tag{8}$$

$$\begin{aligned} x_i^* x_j^* &= (x_i - 2h\delta_{i3})(x_j - 2h\delta_{j3}) \\ &= x_i x_j - 2h(x_i \delta_{j3} + x_j \delta_{i3}) + 4h^2 \delta_{i3} \delta_{j3}. \end{aligned} \tag{9}$$

These relations will be used in the remaining sections.

In [1] it was shown that the system of images for the regularized Stokeslet required the use of two different but related regularization functions. The reason is that while expressions such as $D_1(r) + 2H_2(r) \equiv 0$ in the singular case, this cancellation does not happen automatically with the regularization. However, the cancellation can be obtained by using one blob for the Stokeslet (H_1 and H_2) and a different blob for the dipole (D_1 and D_2). While this was done in [1] for two specific blobs, we extend that work here by starting from an arbitrary blob and providing a formula for the companion blob.

4. Companion blobs and regularized Green's functions

Consider a regularized Stokeslet with blob ϕ_s . All dipoles and sources will use the companion blob ϕ_d . The remaining elements are derived from these; for example, the doublet is derived from the Stokeslet and therefore also comes from ϕ_s . Once the blob ϕ_s is chosen, the corresponding functions G_s and B_s are derived from it using $\Delta G_s = \phi_s$ and $\Delta B_s = G_s$. Similar formulas hold for the triplet (ϕ_d, G_d, B_d) . Assume that (ϕ_d, G_d, B_d) are known. We define the blob ϕ_s using the formula

$$\phi_s = \frac{1}{2}(r\phi_d' + 5\phi_d)$$

which will ensure the appropriate cancellation formulas needed for the images (see Appendix A). In particular, the following proposition, proven in Appendix A, holds:

Proposition 1. *Let the dipole and source be derived from ϕ_d and the Stokeslet from ϕ_s . Then $2H_1'/r + 4H_2 + D_1 = 0$ and $D_2 + 2H_2'/r = 0$.*

Examples of blobs $\phi_d(r)$ and $\phi_s(r)$ are shown in Table 1.

4.1. Relations between the doublet and the dipole kernels

Using Proposition 1, the doublet expression can be simplified

$$\begin{aligned}
\Delta_{ijk} &= \frac{\partial}{\partial x_k} [H_1 \delta_{ij} + x_i x_j H_2] \\
&= \frac{H_1'}{r} x_k \delta_{ij} + H_2 (\delta_{ik} x_j + \delta_{jk} x_i) + \frac{H_2'}{r} x_i x_j x_k \\
&= -\frac{1}{2} (D_1 + 4H_2) x_k \delta_{ij} + H_2 (\delta_{ik} x_j + \delta_{jk} x_i) - \frac{1}{2} x_k x_i x_j D_2
\end{aligned}$$

which leads to the useful identity

$$\Delta_{ijk} + \frac{1}{2} x_k D_{ij} = -2H_2 x_k \delta_{ij} + H_2 (\delta_{ik} x_j + \delta_{jk} x_i). \quad (10)$$

5. The image system for regularized elements

5.1. The images for a regularized Stokeslet

Consider a Stokeslet of strength \mathbf{f} derived from a blob ϕ_s . From the notation in Fig. 1 and Eqs. (8)–(9), we note that when the evaluation point is on the wall, we have $|\mathbf{x}^*| = |\mathbf{x}|$. The fluid velocity evaluated on the wall due to the original Stokeslet and its negative at the image point is

$$\begin{aligned}
(S_{ij}^* - S_{ij}) f_j &= (-2hH_2(x_i \delta_{j3} + x_j \delta_{i3}) + 4h^2 H_2 \delta_{i3} \delta_{j3}) f_j \\
&= -2hH_2 f_3 (x_1 \delta_{i1} + x_2 \delta_{i2}) - 2hH_2 (x_1 f_1 + x_2 f_2) \delta_{i3},
\end{aligned} \quad (11)$$

where H_1 and H_2 are defined in Eq. (5).

We now define a dipole from ϕ_d . The operator $(\Delta_{i3j} + (h/2)D_{ij})$ applied to $2hq_j$ gives

$$\begin{aligned}
2h \left(\Delta_{i3j} + \frac{h}{2} D_{ij} \right) q_j &= h^2 (2H_2 + D_1) q_i + 2hH_2 x_i q_3 - h(D_1 + 4H_2) (x_1 q_1 + x_2 q_2 + hq_3) \delta_{i3} \\
&= h^2 (2H_2 + D_1) (q_1 \delta_{i1} + q_2 \delta_{i2}) + 2hH_2 q_3 (x_1 \delta_{i1} + x_2 \delta_{i2}) \\
&\quad - h(D_1 + 4H_2) (x_1 q_1 + x_2 q_2) \delta_{i3}.
\end{aligned}$$

A linear combination of the last equation and Eq. (11) is not enough to cancel the velocity at the wall as it is in the singular case. As in [1] we consider the difference of two rotlets

$$\mathcal{R}_d - \mathcal{R}_s = \frac{G'_d}{r} - \frac{G'_s}{r} = -\frac{1}{2} D_1 - H_2 \quad (12)$$

where we used the results of Proposition 1 and Theorem 1 (see Appendix A).

If we define the rotlet strength be $L_j = \epsilon_{kj3} q_k$, then from Eq. (12) we have that

$$\begin{aligned}
2h(\mathcal{R}_d - \mathcal{R}_s)_{ij} L_j &= -h(D_1 + 2H_2) \epsilon_{ij\ell} x_\ell \epsilon_{kj3} q_k \\
&= -h(D_1 + 2H_2) \epsilon_{jil} \epsilon_{jk3} x_\ell q_k \\
&= -h(D_1 + 2H_2) (\delta_{ik} \delta_{\ell 3} - \delta_{i3} \delta_{\ell k}) x_\ell q_k \\
&= -h(D_1 + 2H_2) (q_i \delta_{\ell 3} - \delta_{i3} q_\ell) x_\ell \\
&= h(D_1 + 2H_2) \delta_{i3} (q_1 x_1 + q_2 x_2) - h^2 (D_1 + 2H_2) (q_1 \delta_{i1} + q_2 \delta_{i2}).
\end{aligned}$$

Therefore,

$$2h \left(\Delta_{i3j} + \frac{h}{2} D_{ij} \right) q_j + 2h(\mathcal{R}_d - \mathcal{R}_s)_{ij} L_j = 2hH_2 q_3 (x_1 \delta_{i1} + x_2 \delta_{i2}) - 2hH_2 (x_1 q_1 + x_2 q_2) \delta_{i3} \quad (13)$$

Adding Eq. (11) and Eq. (13) we conclude that the velocity field at the wall will vanish when $q_1 = -f_1$, $q_2 = -f_2$ and $q_3 = f_3$, or equivalently, when $q_j = -(\delta_{jk} - 2\delta_{j3}\delta_{k3}) f_k$.

In summary, the image system for a Stokeslet is $u_i = S_{ij}^{IM} f_j$ where

$$S_{ij}^{IM} = (S_{ij}^* - S_{ij}) - 2h\rho_{mj} \left(\Delta_{i3m} + \frac{h}{2} D_{im} \right) - 2h(\mathcal{R}_d - \mathcal{R}_s)_{im} \epsilon_{jm3}$$

where we have defined $\rho_{mj} = (\delta_{mj} - 2\delta_{m3}\delta_{j3})$.

We note that in the singular case, taking the limit as the regularization vanishes, the rotlets cancel each other and the image system for a Stokeslet reduces to

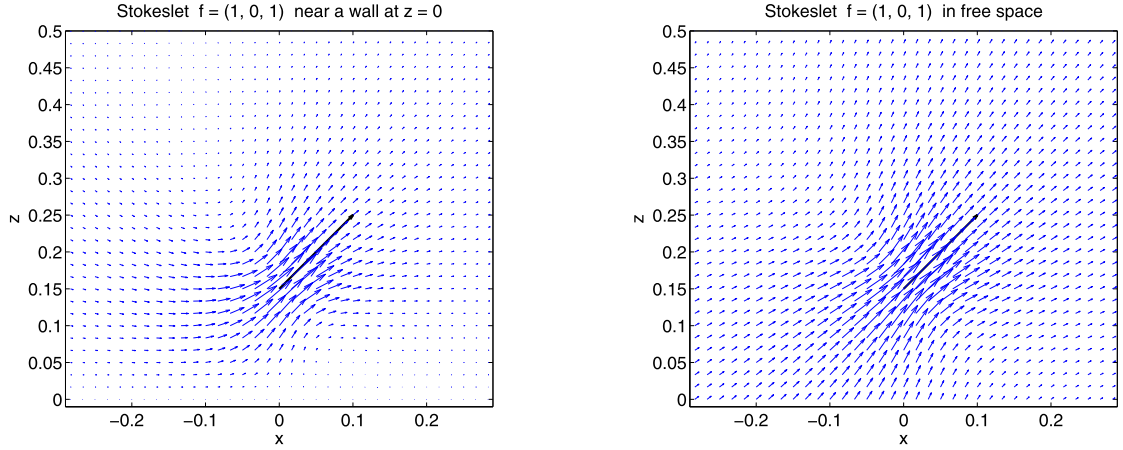


Fig. 2. Flow field due to a Stokeslet near the wall $z=0$ (left) and in free space (right). The blob used is the exponential function in Table 1 and $\delta = 0.014$.

$$\begin{aligned} S_{ij}^{IM} &= (S_{ij}^* - S_{ij}) - \frac{2h\rho_{mj}}{8\pi} \left(\frac{(x_3 - h)\delta_{im} + x_i\delta_{m3} - x_m\delta_{i3}}{r^3} - \frac{3x_mx_i(x_3 - h)}{r^5} \right) \\ &= (S_{ij}^* - S_{ij}) + \frac{2h\rho_{mj}}{8\pi} \frac{\partial}{\partial x_m} \left(\frac{hx_i}{r^3} - \frac{\delta_{i3}}{r} - \frac{x_ix_3}{r^3} \right) \end{aligned}$$

where the last expression is identical to that in [6].

Fig. 2 shows a comparison of the Stokeslet flow with (left) and without (right) images. For the purpose of illustration, the flows in the figures were computed using the exponential blob in Table 1.

5.2. The images for a regularized source

Consider a regularized source (or sink) given in Eq. (4) using the blob $\phi_d(r)$. Using Proposition 1 we find that the fluid velocity at a point on the wall due to the original source of strength 1 and a source at its image is

$$\sigma_i^* + \sigma_i = \Sigma(x_i^* + x_i) = 2\frac{G'_d}{r}(x_i - h\delta_{i3}) = 4H_2(x_i - h\delta_{i3})$$

where H_2 comes from a Stokeslet blob $\phi_s(r)$ as given in Eq. (5). Also, from Eq. (10), the operator $\Delta_{ij3} + (h/2)D_{ij}$ applied to $-4\delta_{j3}$ gives

$$-4\left(\Delta_{ij3} + \frac{h}{2}D_{ij}\right)\delta_{j3} = 8H_2h\delta_{i3} - 4H_2(h\delta_{i3} + x_i) = -4H_2(x_i - h\delta_{i3})$$

from which we conclude that the images of a source of strength m are $u_i = m \sigma_i^{IM}$ where

$$\sigma_i^{IM} = \sigma_i^* + \sigma_i - 4\left(\Delta_{i33} + \frac{h}{2}D_{i3}\right) = 0$$

at every point on the wall.

From this expression one can deduce the singular case by taking the limit as the regularization vanishes. In that case, the image system for a source reduces to

$$\begin{aligned} \sigma_i^{IM} &= \sigma_i^* + \sigma_i - \frac{4}{8\pi} \left(\frac{-h\delta_{i3} + x_i}{r^3} - \frac{3x_3x_i(x_3 - h)}{r^5} \right) \\ &= \sigma_i^* + \sigma_i + \frac{2h}{4\pi} \left(\frac{\delta_{i3}}{r^3} - \frac{3x_3x_i}{r^5} \right) - \frac{2}{4\pi} \left(\frac{x_i}{r^3} - \frac{3x_3x_3x_i}{r^5} \right) \end{aligned}$$

which is the expression derived in [6]. See also [30, p. 197]. Fig. 3 shows a comparison of the source flow with (left) and without (right) images. For this illustration, the flows were computed using the algebraic blob in Table 1.

6. The image systems for other elements

It is known that given the images of a generic element $E_{ij}(\mathbf{x} - \mathbf{x}_0, \delta)$, the corresponding image system for the derivative of that element can be found by differentiating the image system with respect to the pole \mathbf{x}_0 . Here, we will use an equivalent

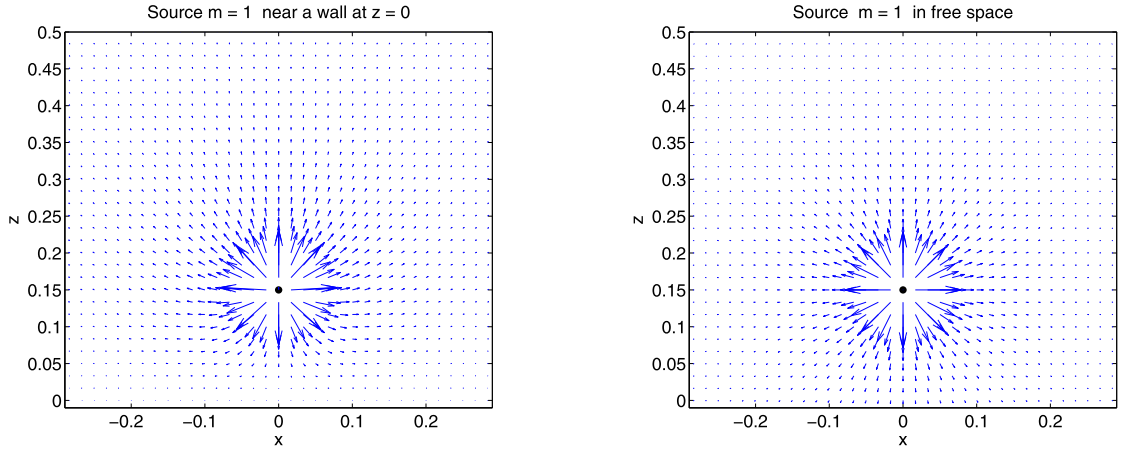


Fig. 3. Flow field due to a source near a wall at $z = 0$ (left) and in free space (right). The blob used is the algebraic function in Table 1 and $\delta = 0.025$.

formula in terms of derivatives with respect to \mathbf{x} . If the image system for $E_{ij}(\mathbf{x} - \mathbf{x}_0, \delta)$ is $h^p F_{ij}(\mathbf{x} - \mathbf{y}_0, \delta)$, then the image system for $\partial E_{ij} / \partial x_k$ is

$$(\delta_{nk} - 2\delta_{n3}\delta_{k3}) \left[\frac{\partial}{\partial x_n} + \delta_{n3} \frac{\partial}{\partial h} \right] (h^p F_{ij}), \quad (14)$$

which can be shown by considering the limiting process of two elements E_{ij} approaching each other. We use this formula in the sections below.

6.1. The images for a regularized dipole

It is easy to check from Eq. (4) and Eq. (7) that the dipole and source are related by $D_{ik} = \phi_d \delta_{ik} - \partial \sigma_i / \partial x_k$, so that in order to derive the image system for a dipole we need to differentiate the image system for the source:

$$\sigma_i - 4 \left(\Delta_{i33} + \frac{h}{2} D_{i3} \right).$$

For notational purposes, we recall that $\rho_{nk} = (\delta_{nk} - 2\delta_{n3}\delta_{k3})$, so we have that the image system of D_{ik}^* is

$$\begin{aligned} & -\phi_d \delta_{ik} - \rho_{nk} \left[\frac{\partial}{\partial x_n} + \delta_{n3} \frac{\partial}{\partial h} \right] \left(\sigma_i - 4 \left(\Delta_{i33} + \frac{h}{2} D_{i3} \right) \right) \\ &= -\phi_d \delta_{ik} - \rho_{nk} \frac{\partial \sigma_i}{\partial x_n} + 4 \rho_{nk} \frac{\partial}{\partial x_n} \left(\Delta_{i33} + \frac{h}{2} D_{i3} \right) + 2 \rho_{nk} \delta_{n3} D_{i3} \\ &= -\phi_d \delta_{ik} - \rho_{nk} \frac{\partial \sigma_i}{\partial x_n} + 4 \rho_{nk} \left(S_{i33n}^Q + \frac{h}{2} Q_{i3n} \right) + 2 \rho_{nk} \delta_{n3} D_{i3} \\ &= -\phi_d \delta_{ik} + \rho_{nk} \left\{ -\frac{\partial \sigma_i}{\partial x_n} + 4 \left(S_{i33n}^Q + \frac{h}{2} Q_{i3n} + \frac{1}{2} \delta_{n3} D_{i3} \right) \right\}. \end{aligned}$$

Now we simplify the last term to get that the image system of a dipole is $u_i = D_{ik}^{IM} f_k$, where

$$D_{ik}^{IM} = D_{ik}^* + \rho_{nk} \left\{ D_{in} + 4 \left(S_{i33n}^Q + \frac{h}{2} Q_{i3n} \right) \right\} - 2\delta_{k3} D_{i3} - (\rho_{ik} + \delta_{ik}) \phi_d,$$

where we have used the quadrupole Q and Stokes quadrupole S^Q defined in Section 2.

As $\delta \rightarrow 0$, this agrees with the known image system in the singular case [30], except for the last term, which approaches a delta distribution. This term has no effect on the fluid motion since it is centered at the image point (outside the fluid domain). We also point out that the image system can be written using different combinations of elements that give the same result. For example, one can verify that the following is an equivalent representation of the image system for the dipole

$$D_{ik}^{IM} = (D_{ik}^* - D_{ik}) + 4 \left(S_{in33}^Q + \frac{h}{2} Q_{in3} + \frac{1}{2} D_{in} \right) \rho_{nk} + 4 \Theta_{i\ell 3}^d \epsilon_{k\ell 3},$$

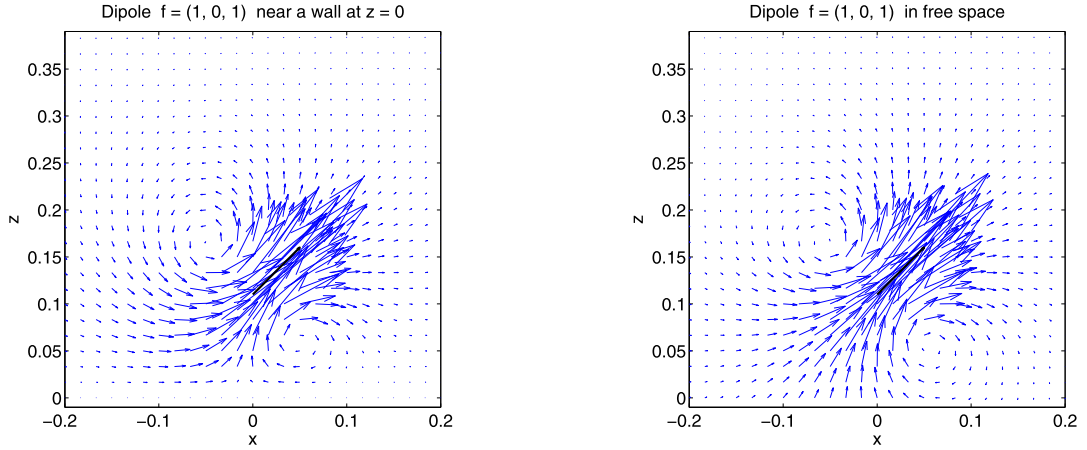


Fig. 4. Flow field due to a dipole near a wall at $z = 0$ (left) and in free space (right). The blob used is the exponential function in Table 1 and $\delta = 0.017$.

which uses also a rotlet double Θ^d derived from ϕ_d . Fig. 4 shows a comparison of the dipole flow with (left) and without (right) images. For this illustration, the flows were computed using the exponential blob in Table 1.

6.2. The images for a regularized doublet

Following the derivation of the dipole system of images, the corresponding system for a doublet can be obtained by differentiating the Stokeslet. We start with the Stokeslet image system

$$-S_{ij} - 2\rho_{mj} \left(h\Delta_{i3m} + \frac{h^2}{2} D_{im} + h(\mathcal{R}_d - \mathcal{R}_s)_{ip} \epsilon_{mp3} \right)$$

and since the doublet is $\Delta_{ijk} = \partial S_{ij} / \partial x_k$, we have that the image system for Δ_{ijk}^* is

$$\begin{aligned} & -\rho_{kn} \Delta_{ijn} - 2\rho_{kn} \rho_{mj} \left[\frac{\partial}{\partial x_n} + \delta_{n3} \frac{\partial}{\partial h} \right] \left(h\Delta_{i3m} + \frac{h^2}{2} D_{im} + h(\mathcal{R}_d - \mathcal{R}_s)_{ip} \epsilon_{mp3} \right) \\ & = -\rho_{kn} \Delta_{ijn} - 2\rho_{kn} \rho_{mj} \left(hS_{i3mn}^Q + \frac{h^2}{2} Q_{imn} + h(\Theta_d - \Theta_s)_{ipn} \epsilon_{mp3} \right) \\ & \quad + 2\rho_{mj} \delta_{k3} (\Delta_{i3m} + hD_{im} + (\mathcal{R}_d - \mathcal{R}_s)_{ip} \epsilon_{mp3}) \end{aligned}$$

so that the system of images for the doublet is

$$\begin{aligned} \Delta_{ijk}^{IM} & = \Delta_{ijk}^* - \Delta_{ijk} - 2\rho_{kn} \rho_{mj} \left(hS_{i3mn}^Q + \frac{h^2}{2} Q_{imn} \right) + 2\delta_{k3} \Delta_{ij3} + 2\rho_{mj} \delta_{k3} (\Delta_{i3m} + hD_{im}) \\ & \quad + 2\epsilon_{jp3} [\delta_{k3} (\mathcal{R}_d - \mathcal{R}_s)_{ip} - h\rho_{kn} (\Theta_d - \Theta_s)_{ipn}] \end{aligned}$$

6.2.1. The images for a regularized rotlet

To find the system of images for a rotlet L , we just need to determine the antisymmetric part of the doublet image system. The result is

$$\begin{aligned} \mathcal{R}_{ij}^{IM} & = (\mathcal{R}_s^* - \mathcal{R}_s)_{ij} L_j - 2(\Delta_{ij3} + \Delta_{i3j} + hD_{ij}) p_j - 2(\mathcal{R}_d - \mathcal{R}_s)_{ij} q_j \\ & \quad - 2h(\Theta_d - \Theta_s)_{ij3} L_j - \frac{h^2}{2} (Q_{ijk} - Q_{ikj}) A_{kj} \end{aligned}$$

where $A_{kj} = \epsilon_{kjl} L_l$, $p_j = \epsilon_{jk3} L_k = A_{3j}$ and $q_j = \epsilon_{j3k} p_k$. Fig. 5 shows a comparison of the rotlet flow with (left) and without (right) images. For this illustration, the flows were computed using the algebraic blob in Table 1.

6.2.2. The images for a regularized stresslet

Given the image system of a full doublet and those of a rotlet and source, the system for a stresslet of strength Z_{jk} (symmetric) is obtained simply by subtracting the appropriate pieces. The result is $u_i = T_{ijk}^{IM} Z_{jk}$ where

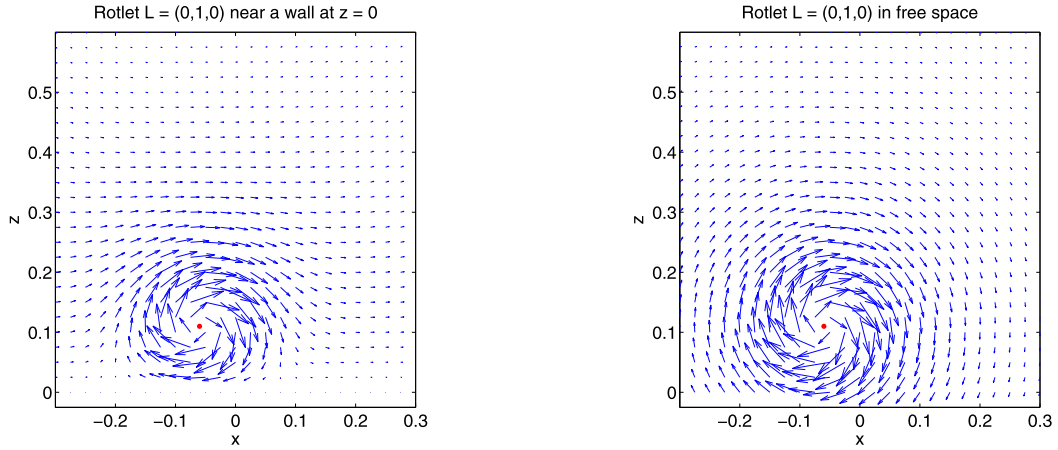


Fig. 5. Flow field due to a rotlet near a wall at $z = 0$ (left) and in free space (right). The blob used is the algebraic function in Table 1 and $\delta = 0.1$.

$$\begin{aligned}
 T_{ijk}^{IM} = & (T_{ijk}^* - T_{ijk}) - 2H_2\delta_{jk}x_i - 2\rho_{kn}\rho_{mj} \left(hS_{i3mn}^Q + \frac{h^2}{2}Q_{imn} \right) \\
 & + 2\delta_{k3}\Delta_{ij3} + 2\delta_{k3}\rho_{jm}(\Delta_{i3m} + hD_{im}) + 2\delta_{jk} \left(\Delta_{i33} + \frac{h}{2}D_{i3} \right) \\
 & - 2h\rho_{nk}(\Theta_d - \Theta_s)_{ipn} \epsilon_{jp3} + 2\delta_{k3}(\mathcal{R}_d - \mathcal{R}_s)_{ip} \epsilon_{jp3}
 \end{aligned}$$

We make the following definitions: (a) $\text{Tr}(Z) = \delta_{jk}Z_{jk}$, (b) $p_j = x_k Z_{jk}$, and (c) $q_j = Z_{j3} = Z_{3j}$ and note that $\mathbf{x} \cdot \mathbf{q} = p_3$. Using this notation, we have that

$$\begin{aligned}
 T_{ijk}^{IM} Z_{jk} = & (T_{ijk}^* - T_{ijk})Z_{jk} - 2H_2x_i \text{Tr}(Z) - 2h \left(S_{i3mn}^Q + \frac{h}{2}Q_{imn} \right) Z_{mn} \\
 & + 8h(S_{i3m3}^Q q_m - S_{i333}^Q q_3) + 4h^2 \left(\frac{1}{2}(Q_{im3} + Q_{i3m})q_m - Q_{i33}q_3 \right) \\
 & + 2\Delta_{ij3}q_j + 2(\Delta_{i3m}q_m - 2\Delta_{i33}q_3) + 2h(D_{im}q_m - 2D_{i3}q_3) \\
 & + 2 \left(\Delta_{i33} + \frac{h}{2}D_{i3} \right) \text{Tr}(Z) - 2h\rho_{nk}(\Theta_d - \Theta_s)_{ipn} \epsilon_{jp3} Z_{jk} + 2(\mathcal{R}_d - \mathcal{R}_s)_{ip} \epsilon_{jp3} q_j.
 \end{aligned}$$

7. Application to cilia motion

We use the method of images for regularized Stokeslets to compute the flow generated by three cilia beating in the same plane at different phases of their motion. This problem has been studied by several investigators (see for example [36] and the references therein). Our goal is not to study this problem in depth but to illustrate the use of regularized images.

The time-dependent shape of a cilium has been approximated by a curve $\xi(s, t)$ in three dimensions given by

$$\xi(s, t) = \frac{1}{2}\mathbf{a}_0(s) + \sum_{n=1}^6 \mathbf{a}_n(s) \cos(n\sigma t) + \mathbf{b}_n(s) \sin(n\sigma t)$$

where s is the arc length parameter and t is time. The coefficients \mathbf{a}_n and \mathbf{b}_n are provided in [32,19]. Here, we scale the cilium to have unit length and set the frequency $\sigma = 1$. The velocity at any point on the cilium at time t can be computed as $\mathbf{v}(s, t) = \partial \xi(s, t) / \partial t$. The flow field everywhere is computed as follows:

1. Discretize the cilium at time t with $\xi_k = \xi(s_k, t)$ for $k = 1, 2, \dots, N$ and compute their corresponding velocities $\mathbf{v}_k = \mathbf{v}(s_k, t)$.
2. If we consider applying a force \mathbf{f}_k at ξ_k , then the fluid velocity \mathbf{v}_i is

$$\mathbf{v}_i = \sum_{k=1}^N S^{IM}(\xi_i, \xi_k) \mathbf{f}_k \tag{15}$$

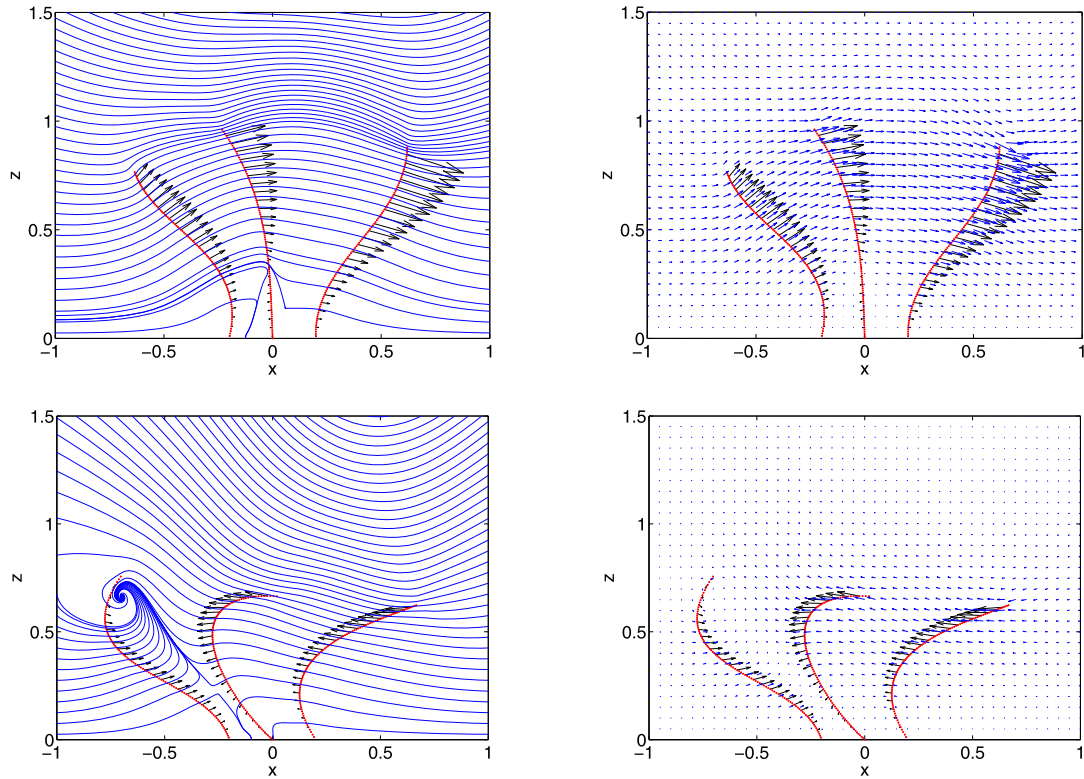


Fig. 6. Example of the use of the image system for regularized Stokeslets in the simulation of three cilia in close proximity to one another. The top row shows streamlines (left) and flow field (right) generated by the cilia at different times during the power stroke. The bottom row shows streamlines (left) and flow field (right) generated by the cilia at different times during the recovery stroke. In all cases, the arrows attached to the cilia represent the imposed velocity. The panels on the right column use the same scale of the velocity field on the plane of the cilia beat for comparison.

where $S^{IM}(\xi_i, \xi_k)$ is a 3×3 matrix representing the image system for the Stokeslets. Enforcing Eq. (15) for $i = 1, 2, \dots, N$ leads to a linear system of $3N$ equations that is solved for the cilium forces.

3. Once the forces are found, the fluid velocity at an arbitrary point \mathbf{x} is computed using $\mathbf{u}(\mathbf{x}) = \sum_{k=1}^N S^{IM}(\mathbf{x}, \xi_k) \mathbf{f}_k$.

In Fig. 6 we have followed this procedure for three cilia simultaneously 0.2 dimensionless units apart at the wall, which is at $z = 0$. The top row of the figure shows cilia whose shape and velocity were computed using $t = 2\pi/13$ (left), $t = 4\pi/13$ (middle) and $t = 6\pi/13$ (right), which are during the power stroke. The bottom row of the figure shows cilia whose shape and velocity were computed using $t = 14\pi/13$ (left), $t = 20\pi/13$ (middle) and $t = 2\pi$ (right), which are during the recovery stroke.

The entire beat of the cilia is in the plane $y = 0$ and the fluid velocity in that plane is also shown in Fig. 6 as streamlines (left column) and as vectors (right column). The arrows attached to the cilia represent the imposed cilium velocity. The Gaussian blob in Table 1 was used in this example.

8. Conclusions

The systematic derivation of the Stokes velocity field due to regularized forces or torques has been useful in modeling biological flows such as those around flagella, spirochetes, and cilia. In order to use these techniques in cases when the flow is bounded by a plane wall, a system of images for each type of singularity must be developed. This had been done previously for the regularized Stokeslet but limited to a specific blob. We have extended that work by deriving the Stokeslet image system for any blob so that it can be used in applications known to require specialized blobs with particular decay properties. We have also extended previous work by presenting the derivation of the system of images for regularized sources, dipoles, rotlets, and stresslets, starting with arbitrary blobs. The image systems have the property that the resulting velocity field is zero analytically at the wall. A feature in the image systems is that two different but related blobs are necessary in the regularization of Stokeslets and dipoles/sources, respectively. We have given explicit formulas that relate the two companion blobs. A direct consequence of this work is the image system for the corresponding standard (singular) elements which are obtained by taking the limit as the regularization parameter δ approaches zero.

Acknowledgements

R. Cortez was partially funded by NSF grant DMS-1217223.

Appendix A

Given the triplet $(\phi_{\delta_d}, G_d, B_d)$, consider the definition of B_s as the solution of

$$\frac{1}{r} \frac{dB_s}{dr} = \frac{1}{2} G_d. \quad (16)$$

This will imply that

$$G_s = \frac{d^2 B_s}{dr^2} + \frac{2}{r} \frac{dB_s}{dr} = \frac{1}{2} \left(r \frac{dG_d}{dr} + 3G_d \right). \quad (17)$$

The dipoles and sources derived from ϕ_d are

$$\begin{aligned} D_1 &= \phi_d - \frac{1}{r} \frac{dG_d}{dr} = \frac{d^2 G_d}{dr^2} + \frac{1}{r} \frac{dG_d}{dr} \\ D_2 &= -\frac{1}{r} \frac{d}{dr} \left[\frac{1}{r} \frac{dG_d}{dr} \right] \\ \Sigma &= \frac{1}{r} \frac{dG_d}{dr} \end{aligned}$$

and the Stokeslets are derived from ϕ_s are

$$\begin{aligned} H_1 &= \frac{1}{r} \frac{dB_s}{dr} - G_s \\ H_2 &= \frac{1}{r} \frac{d}{dr} \left[\frac{1}{r} \frac{dB_s}{dr} \right]. \end{aligned}$$

Using Eqs. (16)–(17) one can prove the following proposition.

Proposition 1. *Let the dipole and source be derived from ϕ_d and the Stokeslet from ϕ_s . Then*

- (a) $2H_1'/r + 4H_2 + D_1 = 0$
- (b) $D_2 + 2H_2'/r = 0$

Proof. To prove (b) we see that from Eq. (16) we have

$$H_2 = \frac{1}{r} \frac{d}{dr} \left[\frac{1}{r} \frac{dB_s}{dr} \right] = \frac{1}{2r} \frac{dG_d}{dr} = \frac{1}{2} \frac{G_d'}{r} \Rightarrow 2H_2 = \frac{G_d'}{r}.$$

This implies that

$$D_2 = -\frac{1}{r} \frac{d}{dr} \left[\frac{1}{r} \frac{dG_d}{dr} \right] = -2 \frac{H_2'}{r}.$$

To prove (a) we see that

$$H_1 = \frac{1}{2} G_d - G_s \Rightarrow \frac{H_1'}{r} = \frac{1}{2} \frac{G_d'}{r} - \frac{G_s'}{r}$$

and using Eq. (17) we can verify that $2H_1'/r + 4H_2 + D_1 = 0$. \square

The proof of Proposition 1 shows that $H_2(r) = \frac{1}{2} \frac{G_d'(r)}{r} = \frac{1}{2} \Sigma(r)$. This is why the first term on the right side of the stresslet velocity in Eq. (6), $H_2(r)(\delta_{jk} Z_{jk})\mathbf{x}$, is equivalent to a regularized source. The same is true without regularization. What remains now is to find the triple (ϕ_s, G_s, B_s) from the known functions (ϕ_d, G_d, B_d) and Eq. (16). The result is

Theorem 1. *Given differentiable functions (ϕ_d, G_d, B_d) , assume the blob decays fast enough that $\lim_{r \rightarrow \infty} r^3 \phi_d(r) = 0$. Let $B_s = \frac{1}{2}(rB_d'(r) + B_d)$. Then, the companion functions satisfy*

$$\frac{1}{r} B'_s(r) = \frac{1}{2} G_d \tag{18}$$

$$\phi_s = \frac{1}{2} (r\phi'_d(r) + 5\phi_d) \tag{19}$$

$$G_s = \frac{1}{2} (rG'_d(r) + 3G_d) \tag{20}$$

Proof. Given the formula for B_s one can see that

$$B'_s = \frac{1}{2} (rB''_d + 2B'_d) = \frac{1}{2} rG_d$$

so that Eq. (18) is satisfied. To establish Eq. (19), note that

$$B''_s = \frac{1}{2} (rG'_d + G_d)$$

so that

$$G_s = B''_s + \frac{2}{r} B'_s = \frac{1}{2} (rG'_d + 3G_d). \quad \square$$

Similarly, one can prove the validity of the formula for ϕ_s . To verify that ϕ_s is a valid blob, we define the n th moment of ϕ as

$$\mathcal{M}_n(\phi) = 4\pi \int_0^\infty r^{n+2} \phi(r) dr$$

and compute (assuming the integrals converge)

$$\begin{aligned} \mathcal{M}_n(\phi_s) &= 4\pi \int_0^\infty r^{n+2} \phi_s(r) dr = 2\pi \int_0^\infty r^{n+3} \phi'_d dr + 10\pi \int_0^\infty r^{n+2} \phi_d(r) dr \\ &= 2\pi (2-n) \int_0^\infty r^{n+2} \phi_d(r) dr + 2\pi \lim_{r \rightarrow \infty} r^{n+3} \phi_d(r) \\ &= 2\pi (2-n) \int_0^\infty r^{n+2} \phi_d(r) dr = \frac{2-n}{2} \mathcal{M}_n(\phi_d) \end{aligned}$$

as long as the functions decay fast enough as $r \rightarrow \infty$. This formula shows that the total integral of ϕ_s is equal to the total integral of ϕ_d (i.e. $\mathcal{M}_0(\phi_s) = \mathcal{M}_0(\phi_d) = 1$) so that ϕ_s is a valid blob. We note that as long as $\mathcal{M}_2(\phi_d) < \infty$, the formula also shows that $\mathcal{M}_2(\phi_s) = 0$ automatically, regardless of the corresponding value for ϕ_d and that higher moments of the two functions are proportional to each other. The relationships of Theorem 1 can be inverted to give the following result.

Corollary 1. Given (ϕ_s, G_s, B_s) the companion functions are given by

$$\phi_d(r) = \frac{2}{r^5} \int_0^r q^4 \phi_s(q) dq, \quad G_d(r) = \frac{2}{r^3} \int_0^r q^2 G_s(q) dq, \quad B_d(r) = \frac{2}{r} \int_0^r B_s(q) dq$$

References

[1] J. Ainley, S. Durken, R. Embid, P. Boindala, R. Cortez, The method of images for regularized Stokeslets, *J. Comput. Phys.* 227 (2008) 4600–4616.
 [2] V. Aranda, R. Cortez, L. Fauci, Stokesian peristaltic pumping in a three-dimensional tube with a phase-shifted asymmetry, *Phys. Fluids* 23 (8) (August 2011) 081901.
 [3] A. Barrero-Gil, The method of fundamental solutions without fictitious boundary for solving Stokes problems, *Comput. Fluids* 62 (2012) 86–90.
 [4] J.T. Beale, A convergent boundary integral method for three-dimensional water waves, *Math. Comput.* 70 (2001) 977–1029.
 [5] J.R. Blake, A Note on the image system for a Stokeslet in a no-slip boundary, *Proc. Camb. Philos. Soc.* 70 (1971) 303.
 [6] J.R. Blake, A.T. Chwang, Fundamental singularities of viscous flow, *J. Eng. Math.* 8 (1) (1974) 23–29.
 [7] E. Bouzarth, M.L. Minion, A multirate time integrator for regularized Stokeslets, *J. Comput. Phys.* 229 (2010) 4208–4224.
 [8] A.T. Chwang, T.Y. Wu, A note on the helical movements of micro-organisms, *Proc. R. Soc. Lond. B* 178 (1971) 327–346.
 [9] L. Cisneros, R. Cortez, C. Dombrowski, R. Goldstein, J. Kessler, Fluid dynamics of self-propelled organisms, from individuals to concentrated population, *Exp. Fluids* 43 (2007) 737–753.

- [10] L. Cisneros, J. Kessler, R. Ortiz, R. Cortez, M. Bees, Unexpected bipolar flagellar arrangements and long-range flows driven by bacteria near solid boundaries, *Phys. Rev. Lett.* 101 (16) (2008) 168102.
- [11] N. Cogan, Two-fluid model of biofilm disinfection, *Bull. Math. Biol.* 70 (2008) 800–819, <http://dx.doi.org/10.1007/s11538-007-9280-3>.
- [12] N. Cogan, R. Cortez, L. Fauci, Modeling physiological resistance in bacterial biofilms, *Bull. Math. Biol.* 67 (4) (2005) 831–853.
- [13] N.G. Cogan, Shankar Chellam, Regularized Stokeslets solution for 2-d flow in dead-end microfiltration: application to bacterial deposition and fouling, *J. Membr. Sci.* 318 (1–2) (2008) 379–386.
- [14] R. Cortez, The method of regularized Stokeslets, *SIAM J. Sci. Comput.* 23 (4) (2001) 1204–1225 (electronic).
- [15] R. Cortez, L. Fauci, A. Medovikov, The method of regularized Stokeslets in three dimensions: analysis, validation and application to helical swimming, *Phys. Fluids* 17 (2005) 1–14.
- [16] Ricardo Cortez, Franz Hoffmann, A fast numerical method for computing doubly-periodic regularized Stokes flow in 3d, *J. Comput. Phys.* 258 (2014) 1–14.
- [17] C. Dombrowski, L. Cisneros, S. Chatkaew, R. Goldstein, J. Kessler, Self-concentration and large-scale coherence in bacterial dynamics, *Phys. Rev. Lett.* 93 (9) (2004) 098103.
- [18] H. Flores, E. Lobaton, S. Mendez-Diez, S. Tlupova, R. Cortez, A study of bacterial flagellar bundling, *Bull. Math. Biol.* 67 (2005) 137–168.
- [19] G.R. Fulford, J.R. Blake, Muco-ciliary transport in the lung, *J. Theor. Biol.* 121 (1986) 381–402.
- [20] J.G. Gibbs, S. Kothari, D. Saintillan, Y.-P. Zhao, Geometrically designing the kinematic behavior of catalytic nanomotors, *Nano Lett.* 11 (6) (2011) 2543–2550.
- [21] E.A. Gillies, R.M. Cannon, R.B. Green, A.A. Pacey, Hydrodynamic propulsion of human sperm, *J. Fluid Mech.* 625 (2009) 445–474.
- [22] S. Jung, K. Mareck, L. Fauci, M. Shelley, Rotational dynamics of a superhelix towed in a Stokes fluid, *Phys. Fluids* 19 (2007) 103105.
- [23] J.O. Kessler, R. Cortez, Flows and transverse forces of self-propelled microswimmers, in: 58th Annual Meeting of the Division of Fluid Dynamics, American Physical Society, Nov. 20–22, 2005.
- [24] A.M. Lee, M.A. Berny-Lang, S. Liao, E. Kanso, P. Kuhn, O.J.T. McCarty, P.K. Newton, A low-dimensional deformation model for cancer cells in flow, *Phys. Fluids* 24 (8) (2012).
- [25] Karin Leiderman, Elizabeth L. Bouzarth, Ricardo Cortez, Anita T. Layton, A regularization method for the numerical solution of periodic Stokes flow, *J. Comput. Phys.* 236 (2013) 187–202.
- [26] E.J. Lobaton, A.M. Bayen, Modeling and optimization analysis of a single-flagellum micro-structure through the method of regularized Stokeslets, *IEEE Trans. Control Syst. Technol.* 17 (2009) 907–916.
- [27] V. Mehandia, P.R. Nott, The collective dynamics of self-propelled particles, *J. Fluid Mech.* 595 (2008) 239–264.
- [28] Hoang-Ngan Nguyen, Ricardo Cortez, Reduction of the regularization error of the method of regularized Stokeslets for a rigid object immersed in a three-dimensional Stokes flow, *Commun. Comput. Phys.* 15 (1) (2014) 126–152.
- [29] T.J. Pedley, J. Kessler, A new continuum model for suspensions of gyrotactic micro-organisms, *J. Fluid Mech.* 212 (1990) 155–182.
- [30] C. Pozrikidis, *Boundary Integral and Singularity Methods for Linearized Viscous Flow*, Cambridge Texts in Applied Mathematics, Cambridge University Press, Cambridge, 1992.
- [31] Bian Qian, Hongyuan Jiang, David A. Gagnon, Kenneth S. Breuer, Thomas R. Powers, Minimal model for synchronization induced by hydrodynamic interactions, *Phys. Rev. E* 80 (Dec. 2009) 061919.
- [32] M.J. Sanderson, M.A. Sleight, Ciliary activity of cultured rabbit tracheal epithelium: beat pattern and metachrony, *J. Cell Sci.* 47 (1981) 331–341.
- [33] J. Simons, S. Olson, R. Cortez, L. Fauci, The dynamics of sperm detachment from epithelium in a coupled fluid-biochemical model of hyperactivated motility, *J. Theor. Biol.* 354 (2014) 81–94.
- [34] D.J. Smith, A boundary element regularized Stokeslet method applied to cilia- and flagella-driven flow, *Proc. R. Soc. A* 465 (Dec. 2009) 3605.
- [35] D.J. Smith, J.R. Blake, E.A. Gaffney, Fluid mechanics of nodal flow due to embryonic primary cilia, *J. R. Soc. Interface* 5 (2008) 567–573.
- [36] D.J. Smith, E.A. Gaffney, J.R. Blake, Modelling mucociliary clearance, *Respir. Physiol. Neurobiol.* 163 (1–3) (2008) 178–188, *Respiratory Biomechanics*.